Intercomparisons and Aerosol Calibrations of 12 Commercial Integrating Nephelometers of Three Manufacturers

J. HEINTZENBERG,[a] A. WIEDENSOHLER,[a] T. M. TUCH,[a,b] D. S. COVERT,[c] P. SHERIDAN,[d] J. A. OGREN,[d] J. GRAS,[e] R. NESSLER,[f] C. KLEEFELD,[g] N. KALIVITIS,[h] V. AALTONEN,[i] R.-T. WILHELM,[j] AND M. HAVLICEK[k]

[a] *Leibniz Institute for Tropospheric Research, Leipzig, Germany*
[b] *Centre for Environmental Research, Department for Human Exposure Research and Epidemiology, Leipzig, Germany*
[c] *Department of Atmospheric Science, University of Washington, Seattle, Washington*
[d] *NOAA/Climate Monitoring and Diagnostics Laboratory, Boulder, Colorado*
[e] *CSIRO Atmospheric Research, Aspendale, Victoria, Australia*
[f] *Laboratory for Atmospheric Chemistry, Paul Scherrer Institute, Villigen, Switzerland*
[g] *Department of Experimental Physics, National University of Ireland, Galway, Galway, Ireland*
[h] *Department of Chemistry, University of Crete, Heraklion, Greece*
[i] *Finnish Meteorological Institute, Helsinki, Finland*
[j] *Meteorological Observatory Hohenpeissenberg, Deutscher Wetterdienst, Hohenpeissenberg, Germany*
[k] *TSI, Incorporated, St. Paul, Minnesota*

(Manuscript received 22 July 2005, in final form 12 December 2005)

ABSTRACT

This study determined measured and Mie-calculated angular signal truncations for total and backscatter TSI, Inc., nephelometers, as a function of wavelength and for particles of known size and composition. Except for the total scattering channels, similar agreements as in a previous study of measured and calculated truncations were derived for submicrometer test aerosols. For the first time, instrument responses were also determined for supermicrometer test aerosols up to 1.9 μm in geometric mean diameter. These supermicrometer data confirm the theoretical predictions of strong angular truncations of the total scatter signals in integrating nephelometers due to the limited range of measured forward scattering angles. Truncations up to 60% were determined for the largest measured particles. Rough empirical truncation corrections have been derived from the calibration data for Radiance Research and Ecotech nephelometers for which no detailed response characteristics exist. Intercomparisons of the nephelometers measuring urban atmospheric aerosols yield average deviations of the slope from a 1:1 relation with a TSI reference nephelometer of less than 7%. Average intercepts range between +0.53 and −0.19 Mm^{-1}. For the Radiance Research and Ecotech nephelometers ambient regressions of the Radiance Research and Ecotech instruments with the TSI nephelometer show larger negative intercepts, which are attributed to their less well characterized optics.

1. Introduction

First Lieutenant R. G. Beuttell invented the integrating nephelometer during World War II (Beuttell and Brewer 1949). This instrument optically integrates scattered light in an ingenious way from a volume of air over a wide range of scattering angles to derive the scattering coefficient, ideally over the full necessary range of scattering angles from 0° to 180°. Electronically operated integrating nephelometers have been used widely in visibility monitoring and atmospheric research since the 1950s (Ruppersberg 1959). Many modifications and a large number of applications of this type of instrument emerged over the past 50 yr. Relevant for the present investigation is the addition of a backscatter shutter to measure hemispheric backscatter coefficients (Waggoner et al. 1972). A review of this type of instrument was prepared by Heintzenberg and Charlson (1996). With increasing attention to possible radiative forcing of climate by anthropogenic aerosols (Charlson et al. 1991) this instrument gained a central

Corresponding author address: J. Heintzenberg, Leibniz Institute for Tropospheric Research, Permoserstr. 15, 04318 Leipzig, Germany.
E-mail: jost@tropos.de

position in monitoring climate-related aerosol properties, that is, spectral scattering coefficients and backscattering coefficients.

Early on the systematic limitations of this technique were noted. It is technically not possible to cover the full range of scattering angles, which nephelometer theory requires for accurate measurements of scattering coefficients. The resulting truncation error was mainly studied through numerical simulations with Mie theory (Ensor and Waggoner 1970; Hasan and Lewis 1983; Heintzenberg and Quenzel 1973a; Quenzel 1969; Rabinoff and Herman 1973; and others). Besides an empirical estimate (White et al. 1994), the systematic increase of this truncation with particle size to date only has been addressed theoretically (Heintzenberg and Quenzel 1973b).

First calibrations of an integrating nephelometer with artificial test aerosols were reported by Heintzenberg (1975). They were extended to several well-characterized particle sizes in the submicrometer range by Anderson et al. (1996). Since then new commercial nephelometers have been added to the aerosol instrumentation in, for example, the aerosol program of Global Atmospheric Watch organized by the World Meteorological Organization (WMO; available online at http://www.wmo.ch/web/arep/gaw/gaw_home.html). Thus, there is the need for intercomparisons of the different types of instruments measuring scattering coefficients. In the present study, an intercomparison for 12 nephelometers from three manufacturers was carried out at the World Calibration Center for Physical Aerosol Parameters of the WMO in Leipzig, Germany, hosted by the Leibniz Institute for Tropospheric Research. The intercomparison was complemented by aerosol calibrations of the instruments with well-defined test aerosols. For the first time, this type of calibration was extended into the supermicrometer particle size range to address experimentally the issue of signal truncation with larger particles.

2. Experimental

a. The integrating nephelometers

The bulk of the nephelometers investigated in the present study were the three-wavelength models 3563 (and one single-wavelength model 3561) manufactured by TSI, Inc., St. Paul, Minnesota. The most prominent distinguishing features of the TSI nephelometers are the three wavelengths (450, 550, and 700 nm) and corresponding three backscattering channels following the design of Waggoner et al. (1972). These instruments have been characterized in detail by Anderson et al. (1996). In particular, angular and spectral sensitivities have been measured by Anderson et al. and are used in the Mie calculations of section 3. The most recently delivered TSI instrument at the time of the experiment (series number 1083) was operated as a reference in parallel with each of the other nephelometers through a short manifold.

The Radiance Research M903 integrating nephelometer is produced by Radiance Research, Seattle, Washington. It is a single-wavelength, flash-lamp-illuminated instrument using the geometry of a standard integrating nephelometer. Technical details have not been specified by the manufacturer. The wavelength response of this type of nephelometer varies from instrument to instrument. Some were made with a Wratten filter, which results in ca. 530 nm wavelength. Others were modified with an interference filter (Anderson et al. 2003) and were determined to have an effective wavelength of 543 nm based on spectrophotometer measurements of the combined flash lamp, filter, and detector sensitivity (D. S. Covert 2006, unpublished manuscript).

Ecotech Pty, Ltd., Blackburn, Australia, manufactures the single-wavelength integrating nephelometer model 9003 in green 525-, red 630-, and blue 470-nm wavelength versions; a 525-nm version was available for the intercomparison. According to its manual, the Ecotech nephelometer measures the light-scattering coefficient due to particles using the geometry of a standard integrating nephelometer over the angular range 10°–170°. The light source used in the Ecotech nephelometer is an array of light-emitting diodes (LEDs), housed in a black assembly closed off from the sample cell by a glass diffuser plate. Each LED is focused at the center point of this diffuser, and the drive current to each LED is adjusted individually so that the angular distribution of light approximates a cosine function. D. Logan of Ecotech Pty, Ltd., kindly provided a measured angular distribution of the illumination in this type of nephelometer, which was used in the Mie calculations (cf. section 3).

Light-scattering measurements from all three types of nephelometers are automatically compensated for pressure and temperature changes. Table 1 summarizes the key parameters of all nephelometers in the present study.

Most of the nephelometers tested were removed from active use at Global Atmospheric Watch (GAW) stations and shipped to Leipzig. All nephelometers were unpacked, set up in close proximity to one another, and allowed to run for several hours. For each nephelometer, an initial span gas check was performed where the scattering coefficients of filtered air and filtered CO_2 were determined and compared against literature values. After this initial performance check in

TABLE 1. Characteristics of the intercompared integrating nephelometers; RF_{1083} is the average ratio of the total green scattering signal of the individual nephelometer to the respective signal of the TSI model 3563 model number 1083 measured with submicrometer DEHS aerosols, and RC_{1083} is the corresponding ratio for supermicrometer test aerosols.

Manufacturer	Model	Serial No.	Wavelength(s) (nm)	Angular limits	Backscatter	RF_{1083}	RC_{1083}
TSI, Inc.	3561	1035	550	7°–171°	No	1.10	1.12
TSI, Inc.	3563	1001	450, 550, 700	7°–171°	Yes	1.11	1.05
		1005				1.07	1.10
		1016				1.06	1.10
		1025				1.06	No data
		1027				1.06	1.25
		1032				1.04	1.29
		1061				1.02	1.11
		1062				1.02	1.09
		1083				1.00	1.00
Radiance Research	M903	353	543	10°–170°[a]	No	1.14[c]	
		408	543			1.14[c]	
		ASF	532			1.01[c]	
Ecotech	9003		525[b]	10°–170°[b]	No	1.06[c]	

[a] Estimated from technical drawings.
[b] Manufacturer's information.
[c] In RF_{1083} and RC_{1083} the signal of TSI nephelometer 1083 was linearly interpolated in between its blue and green channels at the wavelength of the individual nephelometer.

the "as received" condition, a complete service was performed on each nephelometer, which included cleaning of the instrument interior, replacing old filters and defective or poorly performing parts, reseating loosely connected components, and performing a new calibration with filtered air and CO_2. After this instrument service, a second span gas check was performed with each nephelometer in "optimized" condition. While some of the nephelometers showed initial span gas errors of >10% (average of all six total and backscatter channels) after shipping, all with the exception of TSI Nephelometer 1061 showed span gas average errors of 2% or less after service. Nephelometer 1061 had to be repaired several times until a final span gas check average error of 1.9% was achieved prior to the instrument intercomparisons.

b. Aerosol generation

Near-monodisperse size distributions of di-ethylhexyl-sebacate (DEHS) droplets were generated with a Monodisperse Aerosol Generator (MAGE; TSI, model 3475). Whereas the number concentration of test particles varied within ±50% of the mean for any given setting of the generator and nephelometer run, the more important mean size of the particles concurrently varied by less than 1%. The complex refractive index m_λ of DEHS is given in Anderson et al. (1996) for the wavelengths of the TSI nephelometers; these values were interpolated to the wavelengths of the other nephelometers using a second-order polynomial fit to the data in Anderson et al. (1996).

Test aerosols were generated in the submicrometer range between 300 and 400 nm to represent the optically most important accumulation range in the atmospheric aerosol, and at supermicrometer diameters between 1100 and 1800 nm for a first experimental evaluation of the angular truncation of the nephelometer signals in the coarse particle range (cf. Table 2).

c. Aerosol number size distributions

Monodisperse particle fractions were selected from the polydisperse DEHS aerosol in the above size ranges by a Hauke-type differential mobility analyzer (DMA) manufactured by IfT (rod length 28 cm). The submicrometer number size distributions of the monodisperse test aerosol were measured using a Scanning Mobility Particle Sizer (SMPS; Wang and Flagan 1990) developed and tested by the Leibniz Institute for Tropospheric Research. The SMPS was operated with a 30-s up- and down-scan rate. Operating parameters of the system were selected in order to reduce concentration and sizing errors due to nonideal transfer functions in an SMPS (Collins et al. 2004). Sheath air was set to 5 L min^{-1} and aerosol flow was set to 0.5 L min^{-1}. A match of up- and down-scan distributions determined the delay time. An arithmetic average of both distributions provided the number size distribution for further calculations. Excess concentrations derived from SMPS measurements compared to measurements by an Ultrafine Condensation Particle Counter TSI UCPC 3025 and were found to be less than 3%.

TABLE 2. Geometric mean diameters (D_{g0}, nm), total number (N, cm^{-3}), and geometric standard deviations (σ_l, σ_r) of left and right wing of a biwinged lognormal fit of the DEHS test size distributions.

	Submicrometer				Supermicrometer			
Nephelometer	D_{g0}	N	σ_l	σ_r	D_{g0}	N	σ_l	σ_r
1001	357	625	1.10	1.13	1367	44	1.11	1.18
1005	358	857	1.10	1.13	1375	28	1.11	1.17
1016	326	2445	1.10	1.14	1381	43	1.12	1.19
1025	359	1160	1.10	1.11	N/A	N/A	N/A	N/A
1027	358	445	1.10	1.13	1757	70	1.07	1.07
1032	357	342	1.10	1.12	1430	46	1.14	1.20
1035	379	2295	1.14	1.12	1733	149	1.07	1.08
1061	387	240	1.09	1.10	1396	37	1.12	1.19
1062	372	2689	1.14	1.12	1374	36	1.11	1.19
1083 (1001)	357	625	1.10	1.13	1372	31	1.11	1.18
1083 (1005)	358	857	1.10	1.13	N/A	N/A	N/A	N/A
1083 (1016)	326	2445	1.10	1.14	N/A	N/A	N/A	N/A
1083 (1025)	359	1160	1.10	1.11	N/A	N/A	N/A	N/A
1083 (1027)	358	445	1.10	1.13	N/A	N/A	N/A	N/A
1083 (1032)	357	342	1.10	1.12	N/A	N/A	N/A	N/A
1083 (1035)	379	2295	1.14	1.12	N/A	N/A	N/A	N/A
1083 (1061)	387	240	1.09	1.10	N/A	N/A	N/A	N/A
1083 (1062)	372	2689	1.14	1.12	N/A	N/A	N/A	N/A
1083 (RR353)	306	3054	1.11	1.15	N/A	N/A	N/A	N/A
1083 (RR408)	295	3013	1.11	1.16	N/A	N/A	N/A	N/A
1083 (RRASF)	316	2687	1.10	1.14	N/A	N/A	N/A	N/A
1083 (Ecotech)	349	3521	1.15	1.12	N/A	N/A	N/A	N/A
RR353	306	3054	1.11	1.15	1865	138	1.08	1.07
RR408	295	3013	1.11	1.16	1827	117	1.08	1.07
RRASF	316	2687	1.10	1.14	1797	147	1.08	1.08
Ecotech	349	3521	1.15	1.12	1768	283	1.07	1.08

Supermicrometer-size distributions were measured with an Aerodynamic Particle Sizer (APS) (TSI model 3310). This instrument is known to undersize liquid drops because of their deformation to oblate spheroids in the accelerating air downstream of the APS nozzle. Undersizing by up to 25% has been reported for drop diameters between 6 and 14 μm (Baron 1986; Marshall et al. 1991), but the undersizing of the APS has not been determined for the 1.1–1.8-μm diameter DEHS drops used in the present study. Thus, we shall report our comparisons of measured and APS-derived light scattering for different values of the undersizing factor in section 5b.

Although number concentrations of the test aerosols were neither highly reproducible nor very stable, the shape of the distribution varied only little and could be approximated better with biwinged lognormal functions than with those having a single geometric standard deviation. However, the geometric standard deviation of the left wing ($\sigma_l = 1.1 \pm 0.02$, uncertainty = one standard deviation) was statistically undistinguishable from that of the right wing ($\sigma_r = 1.13 \pm 0.02$). Geometric mean diameters, total numbers, σ_l, and σ_r are given for each test aerosol in Table 2.

3. Mie calculations

A scattering signal S_λ of an integrating nephelometer at the wavelength λ can be written as

$$S_\lambda = 2\pi \int_{\theta_1=0}^{\theta_2=180} Z_\lambda(\theta) F_\lambda(\theta)\, d\theta, \tag{1}$$

where $Z_\lambda(\Theta)$ represents the angular sensitivity of the instrument and

$$F_\lambda(\theta) = \int_{-\infty}^{+\infty} f_\lambda(\theta, m_\lambda, d_p) \frac{dn(d_p)}{d \log d_p} \pi \left(\frac{d_p}{2}\right)^2 d \log d_p + F_R(\theta) \tag{2}$$

is the total spectral scattering function of the carrier gas and the particle population with number size distribution $[dn(d_p)/d \log d_p]$. The contribution of the carrier gas air $F_R(\Theta)$ to the total scattering function can be calculated analytically by means of the Rayleigh–Cabannes theory (e.g., Kasten 1968) for given pressure and temperature.

The particulate fraction of the total scattering function is the integral of the scattering functions $f_\lambda(\Theta)$ of the individual particles, weighted with their number

concentrations $[dn(d_p)/d\ \log d_p]$ and their geometric cross sections $\pi[(d_p/2)]^2$. For given values of the particle diameter d_p, λ, and the complex refractive index m_λ, $f_\lambda(\Theta)$ was calculated with Mie-scattering routines following Ackerman and Toon (1981) and Dave (1968, 1969).

Nephelometer scattering and backscattering signals were calculated with Eq. (1) at the peak wavelengths λ of the respective instruments from the number size distributions measured by the SMPS or APS. For the TSI nephelometers these wavelengths have been determined by spectrophotometric transmission measurements on the optical filters (Anderson et al. 1996), and the calculations assumed that the optical filters did not change over time. For the other instruments, only nominal manufacturers' wavelengths could be used.

Simulation of nephelometer signals with Mie calculations requires the knowledge of the angular sensitivities $Z_\lambda(\Theta)$ of the instruments for the integration of the scattering function from scattering angle $\Theta_1 = 0°$ to $\Theta_2 = 180°$. Ideally, $Z_\lambda(\Theta)$ equals $\sin(\Theta)$ for all values of Θ and λ. In that case and $\Theta_1 = 0° S_\lambda \equiv \sigma_{s,\lambda}$, the spectral scattering coefficient of the measured aerosol; for $\Theta_1 = 90° S_\lambda \equiv \sigma_{\mathrm{bs},\lambda}$, the spectral backscattering coefficient. The angular sensitivities of the TSI nephelometers for total scatter and backscattering channels have been measured by Anderson et al. (1996), albeit without testing potential wavelength dependencies that may arise, for example, because of spectrally varying wall reflections in the illuminated sensing chamber of the nephelometer. To our knowledge, this has only been done by Heinicke (1967) for modifications of the open-chamber Ruppersberg nephelometer (Ruppersberg 1964), which cannot be compared to the present set of instruments because of strongly differing angular and spectral characteristics. Comparable angular data are not available for the other commercial instruments. For the Radiance Research nephelometer, angular limits of integration of 10° to 170° were estimated from the available technical drawings. Between these nominal angular limits the sensitivities of the Radiance Research instruments were initially assumed to follow the measured TSI sensitivities. Initial Mie calculations for the Ecotech nephelometer used the available angular sensitivity data supplied by the manufacturer.

For the present study, a FORTRAN code was written utilizing the above-mentioned Mie subroutines and integrating Eq. (1) over the angular range from 0° to 180° and Eq. (2) over the measured size distributions. Alternatively, Eq. (1) was integrated over the scattering function of a carrier gas to simulate the nephelometer signal for a gas calibration. All nephelometer signals and scattering coefficients will be reported in units of $10^{-6}\ \mathrm{m}^{-1} = \mathrm{Mm}^{-1}$.

Spectral angular signal truncations of total scatter $T_{t,\lambda}$ and backscatter signals $T_{b,\lambda}$ of an integrating nephelometer are defined as

$$T_{t,\lambda} = \frac{2\pi \int_{\theta=0}^{\theta=180} Z_{t,\lambda}(\theta) F_\lambda(\theta)\, d\theta}{2\pi \int_{\theta=0}^{\theta=180} \sin(\theta) F_\lambda(\theta)\, d\theta} \tag{3a}$$

and

$$T_{b,\lambda} = \frac{2\pi \int_{\theta=0}^{\theta=180} Z_{b,\lambda}(\theta) F_\lambda(\theta)\, d\theta}{2\pi \int_{\theta=90}^{\theta=180} \sin(\theta) F_\lambda(\theta)\, d\theta}, \tag{3b}$$

respectively, with $Z_{t,\lambda}$ being the angular sensitivity for total scatter wavelength λ and $Z_{b,\lambda}$ being the angular sensitivity for the respective backscatter channel. Truncation of the gas calibration signals $T_{t,R}$ and $T_{b,R}$ is calculated in a similar fashion with $F_\lambda(\Theta) = F_R(\Theta)$.

4. Error analysis

Closure between measured optical signals and those Mie calculated from concurrent measurements of size distributions is the basis of well-conducted aerosol–optical intercomparisons (Ogren 1995; Quinn et al. 1996; Wex et al. 2002). For that purpose the uncertainties of measured and calculated properties must be evaluated. Several studies have estimated the total uncertainty in the scattering measurements of the TSI instruments at somewhere around 10% and many of these break the total errors down into their component parts excluding the truncation corrections (Anderson et al. 1999; Masonis et al. 2002; Sheridan et al. 2002). There are no comparable investigations available for the Radiance Research and Ecotech nephelometers. For the TSI nephelometers the following instrumental error analysis follows Anderson et al. (1996) and Anderson and Ogren (1998).

For the closure test the ratio of measured to Mie-calculated nephelometer signals, subsequently denoted RC, was used. Four sources of errors contributed to the uncertainty of the numerator.

1) The relative uncertainty due to photon-counting statistics: Averaged over all available TSI nephelometers it is ~0.1%–0.3% for total scattering channels at 100 Mm^{-1} and ~0.4%–1.0% for backscattering channels at 10 Mm^{-1}. However, the average values in the

individual channels were taken into account in the error propagation.

2) The precision of the determination of zero background signals: The precision of the zero determination over all channels was ~0.04–0.1 Mm^{-1}, which was neglected in the error propagation because of being less than 1% of the smallest measured signal in the respective channel.
3) Errors of the gas calibrations: The mean calibration error was about 1% for the total scatter blue and green channels, but jumps to ~1.8% in the red. Similarly, the blue and green backscattering channels show errors of 1.4%–1.5% whereas the red backscatter had a mean error of ~2.7%. Average errors of the individual channels were taken into account in the error propagation.
4) The measured variability of the nephelometer signals during each scan of the size distribution measurement.

For the uncertainties in the measured size distributions that formed the basis of the Mie-calculated nephelometer signals, 15% in particle counts and 10% in particle diameters are assumed, based on comparisons of DMA-derived total numbers and concurrent CPC measurements and on flow uncertainties in the DMA. For want of similar comparisons with independent instruments the same uncertainties in concentration and size were assumed in the supermicrometer-size range. Within the two uncertainty limits the particle concentrations and diameters of any measured size distribution are varied at random 30 times. For each varied size distribution nephelometer signals were Mie-calculated; average calculated signals and average relative deviations thereof were formed.

With the help of the uncertainty in average ratio RC for any given run the results were screened for outliers. Measured data (nephelometer and size distribution) that contributed more than three standard deviations to the uncertainty of the average ratio RC were discarded.

5. Results and discussion

We discuss separately the laboratory results for the TSI instruments because their optical configuration is best characterized. Based on a comparison with the TSI results, we later derive empirical modifications of the nominal optical characteristics of the other instruments.

a. Submicrometer test aerosols

For the submicrometer test aerosols, all the nephelometers were operated in parallel with the most recent TSI nephelometer (number 1083). Total particle numbers were between 200 and 4000 cm^{-3} with total scattering levels in the midvisible channels around 300 Mm^{-1}. Average ratios of total scatter signals RF_{1083} relative to those for TSI 1083 are reported in Table 1. RF_{1083} is the average ratio of the total green scattering signal of the individual nephelometer to the respective signal of the TSI model 3563 model 1083 measured with submicrometer DEHS aerosols. These ratios vary between 1.02 and 1.11 for the TSI instruments with an average value of $RF_{1083} = 1.06$. These values are mostly within the expected error limits of the instruments (cf. section 4). However, there is a downward trend of RF_{1083} from the oldest (1001) to the newest (1062) TSI nephelometer, which could be due to some change in the shape of the angular or wavelength response. A loss of sensitivity, or slight shift in wavelength of the filter, would largely be reflected in the gas calibration, and would not show up as drift. For the calculation of RF_{1083} of the other instruments, the denominators were interpolated linearly between the blue and green channel averages of 1083 at the respective wavelength of the individual nephelometer. The largest values of RF_{1083} were reached for the Radiance Research instruments ($RF_{1083} = 1.14$), which may suggest a calibration problem.

In the two scatterplots of Figs. 1a,b measured total and backscatter signals of all nephelometers are compared to respective signals calculated via Eq. (1) from the measured size distributions. Each data point represents one experiment, that is, one test aerosol size distribution measured with two nephelometers in parallel and with the SMPS instrument. Error bars indicate the total uncertainties of the respective measured and calculated nephelometer signals according to error propagation specified in section 4.

In general, measured and calculated signals of the TSI nephelometers are highly correlated. Coefficients of determination range between 0.990 (backscatter blue) and 0.996 (total scatter blue). However, a tendency of systematically higher calculated signals as compared to measured ones is visible, in particular at lower particle concentrations and most so in the red total channel. On average, relative to the calculated signals this deviation is −20% in the red total channel (cf. Table 3). This table also gives average relative deviations of all other measured signals from respective calculated ones and a grand average over all channels of 9.7%. This value is more than twice as high as the respective value of 4.0 of Anderson et al. (1996) because they did not see a systematically high deviation in the total red channel. The results in Table 3 for a red wavelength of 770 nm will be discussed in section 5c.

The magnitudes of nephelometer signals depend on

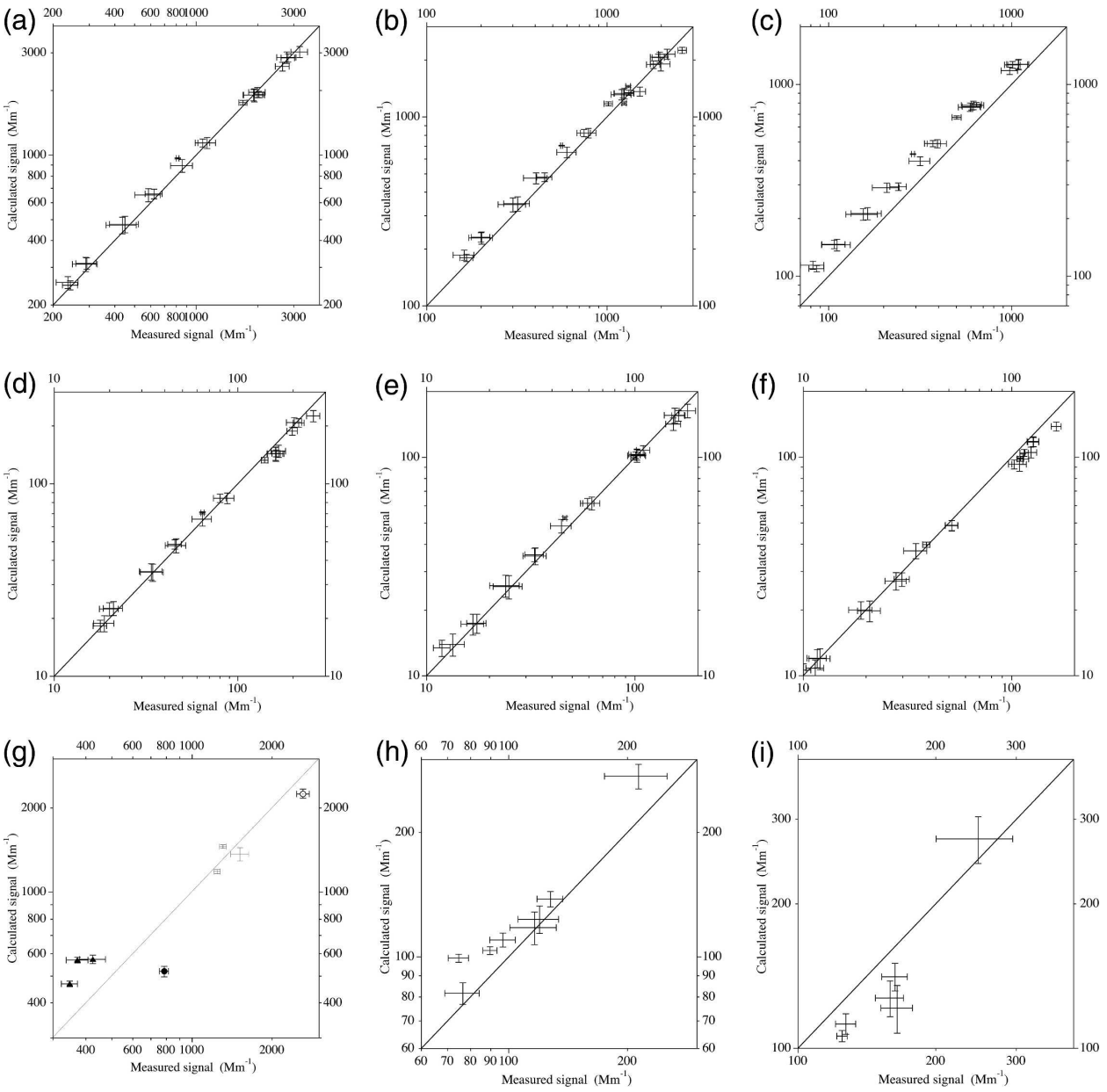

FIG. 1. (a) Scatterplot of average measured and Mie-calculated nephelometer total scatter signals for submicrometer test aerosols and TSI blue signals. Error bars indicate the uncertainties of measured and calculated signals. (b) As in (a) but for TSI green total scatter signals. (c) As in (a) but for TSI red total scatter signals. (d) As in (a) but for TSI blue backscatter signals. (e) As in (a) but for TSI green backscatter signals. (f) As in (a) but for TSI red backscatter signals. (g) Scatterplot of average measured and Mie-calculated nephelometer total scatter signals for Radiance Research submicrometer (cross) and supermicrometer (full triangle) signals and for Ecotech submicrometer (open circle) and supermicrometer (full circle) signals. Error bars indicate the uncertainties of measured and calculated signals. (h) Scatterplot of average measured and Mie-calculated nephelometer total scatter signals for supermicrometer test aerosols and TSI blue signals. Error bars indicate the uncertainties of measured and calculated signals. (i) As in (h) but for TSI green total scatter signals. (j) As in (h) but for TSI red total scatter signals. (k) As in (h) but for TSI blue backscatter signals. (l) As in (h) but for TSI green backscatter signals. (m) As in (h) but for TSI red backscatter signals.

the angular and spectral sensitivities of the instruments. As a test of the correctness of the respective data (or assumptions in the case of Radiance Research and Ecotech) the ratios of measured to calculated signal truncations were calculated according to Eq. (2). In both types of truncations calculated scattering coefficients were employed as denominators. A ratio of one can be interpreted as the angular and spectral sensitivi-

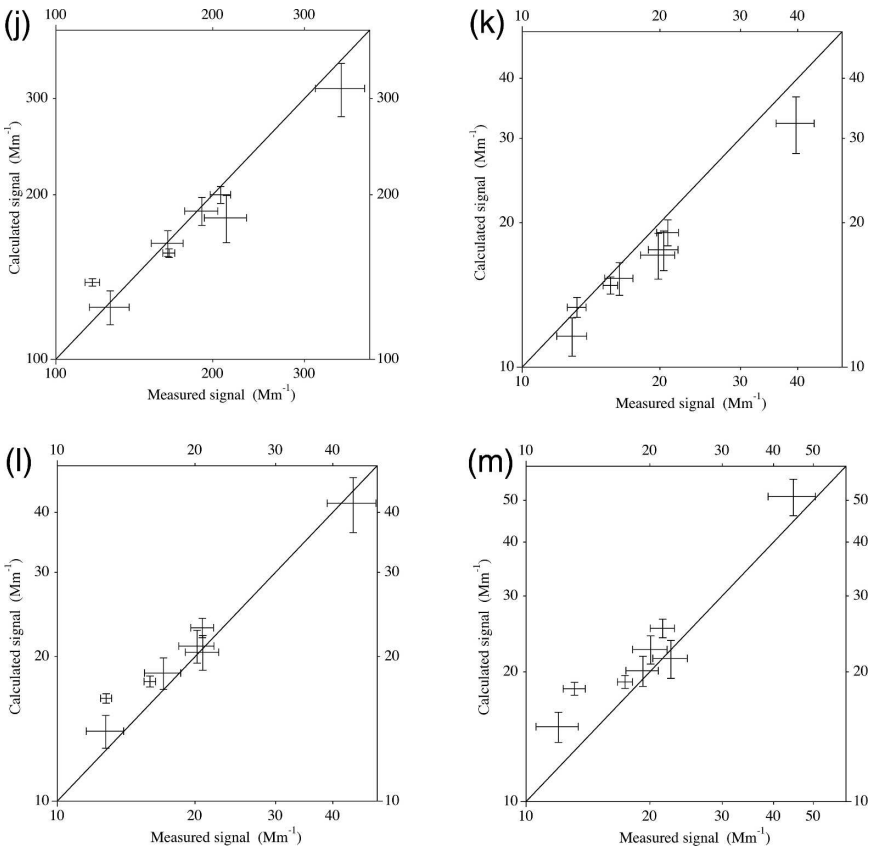

FIG. 1. (*Continued*)

ties correctly reflecting the nephelometer's response. The ratios are plotted in Fig. 2a, which shows separately the average ratios for the nine TSI nephelometers (except 1083), the respective ratios for the 13 experiments in which TSI nephelometer 1083 was operated in parallel with another instrument, average results for the three Radiance Research nephelometers, and the results for the Ecotech instrument. Error bars indicate the variability of the ratios within each group of instruments in terms of a standard deviation. Except for the total red channel the ratios for all instruments lie within 20% of the ideal value of unity. There is a systematic variation of the ratio over the six TSI nephelometer channels, which is very similar for the average of nine different nephelometers and the average of 13 runs with TSI 1083. We interpret this similarity as systematic differences in angular and/or spectral sensitivities in the six channels of all TSI nephelometers that are not described correctly with the available spectral and angular information.

TABLE 3. Average relative deviations in percent of measured signals from respective Mie-calculated scattering signals for the six channels of the TSI nephelometers in Table 1. The results of the present study are compared to those of Anderson et al. (1996) and with those of the present study with a modified red wavelength of 770 nm. GA = Grand average (absolute value) relative deviation over all channels.

Relative deviation	TS blue	TS green	TS red	BS blue	BS green	BS red	GA
Submicrometer							
Present study (700 nm)	−1.1	−5.9	−20.1	4.9	0.5	10.2	9.7
Anderson et al. (1996)	−4.7	−4.6	−2.9	−0.3	−2.3	6.1	4.0
Present study (770 nm)	−1.35	−6.0	2.6	4.6	0.25	6.5	4.3
Supermicrometer							
Present study (700 nm)	−12.7	2.4	5.0	12.4	−4.8	−11.5	9.1
Anderson et al. (1996)	N/A	N/A	N/A	N/A	N/A	N/A	
Present study (770 nm)	−12.9	1.7	4.5	12.4	−3.2	−11.2	8.9

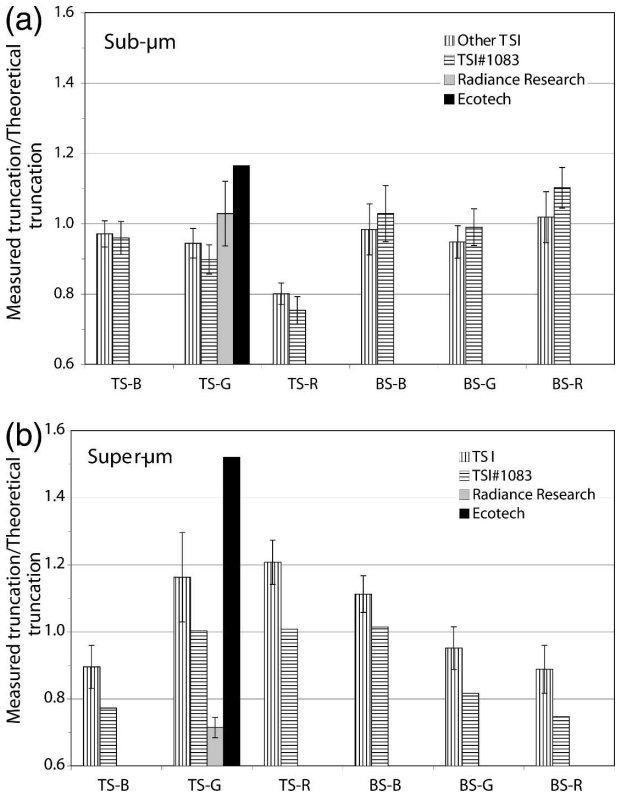

FIG. 2. (a) Average ratios of measured to calculated signal truncations for TSI, Radiance Research, and Ecotech nephelometers and submicrometer DEHS aerosols. TS-B = total scatter blue wavelength, TS-G = total scatter green wavelength, TS-R = total scatter red wavelength, BS-B = backscatter blue wavelength, BS-G = backscatter green wavelength, BS-R = backscatter red wavelength, TSI-Other = TSI nephelometers series number 1001–1062, TSI 1083 = TSI nephelometer series number 1083, Radiance Research = Radiance Research nephelometers, Ecotech = Ecotech nephelometer. Error bars indicate the variability of the individual ratios: TSI-Other = nine TSI nephelometers series number 1001–1062, TSI#1083 = 13 runs of TSI nephelometer series number 1083, Radiance Research = three Radiance Research nephelometer. (b) As in (a) but for supermicrometer DEHS aerosols. Only one run of TSI nephelometer series number 1083 was available.

b. Supermicrometer test aerosols

Total number concentrations in the supermicrometer-size range were 30–300 cm^{-3} with total scattering levels in the midvisible channels between 200 and 400 Mm^{-1}. Because of the low numbers of test particles in the supermicrometer-size range, only one nephelometer was operated at a time. Thus, a direct comparison of instrument readings could not be made. Instead, the readings of the different instruments were normalized by the particle number concentration during the individual tests and then compared to each other. Based on the same procedure as for submicrometer test aerosols, average ratios RC_{1083} are given for the normalized scattering data in Table 1. The RC_{1083} varies between 1.04 and 1.29 for the TSI instruments with an average value of $RC_{1083} = 1.13$. No trend of RC_{1083} with instrument age is visible.

The supermicrometer DEHS number size distributions were measured with an APS. The aerodynamic diameters of this instrument were converted to geometric sizes for the Mie calculations using the density of DEHS. Measured total scattering signals of the TSI nephelometers were roughly 30% higher than those calculated from the size distributions. Some of this difference would be expected from the undersizing of the liquid DEHS particles discussed in section 2c. No experimental means were available to determine the exact undersizing. Instead, an empirical approach was taken by performing the Mie calculations with different values of the assumed undersizing factor. For each value the average ratio of measured total and backscattering signals to respective Mie scattering coefficients was determined. A minimum absolute deviation of both total scattering and backscattering from theoretical values was found for an assumed undersizing of 20%. For this value, the average ratio of measured to Mie-calculated total scattering is 1.05. For backscattering the respective average ratio is 0.96. If the assumed undersizing is 9% (23%), the average ratios become 1.23 (0.97) for total scattering and 1.17 (0.86) for backscattering.

Scatterplots of measured versus calculated nephelometer signals are shown in Figs. 1c,d. Both scatter of the data and uncertainties of the individual points are higher in the supermicrometer range. Because of the large scattering cross sections of the particles, small changes in particle number due to generator instabilities and particle losses have large effects on the measurements. However, also with supermicrometer aerosols, measured and calculated signals of the TSI nephelometers are highly correlated. Coefficients of determination range between 0.954 (total scatter blue) and 0.992 (backscatter blue). No large systematic deviations from the 1:1 line are obvious in Figs. 1c,d. Average relative deviations of measured from calculated signals are listed in Table 3 with a grand average absolute value of 9.1%.

As with the submicrometer test aerosols, the average ratios of measured to calculated truncations in Fig. 2b lie within ±20% of unity. The ratios vary systematically over the six nephelometer channels with highest positive deviations in the red total scattering channel, which is where the largest negative deviation occurred for submicrometer aerosols. In contrast to the submi-

crometer experiments, only one run with the reference nephelometer TSI 1083 was available. Nevertheless, qualitatively, the deviations from expected truncations in TSI 1083 are quite similar over all six channels.

c. Radiance Research and Ecotech instruments

The angular sensitivity curve $Z(\Theta)$ of an integrating nephelometer is the primary parameter that controls (besides the spectral sensitivity) the response of this instrument to particles of different sizes. Two factors control the angular sensitivity curve: the angular limits of integration, defined by the instrument's geometry, and the shape of the curve relating illumination intensity and angle, which ideally is $\sin(\Theta)$. For Radiance Research instruments, $Z(\Theta)$ has not been characterized in detail. When tentatively applying the sensitivity curve of TSI nephelometers within the nominal angular limits (cf. Table 1), the measured truncation for submicrometer particles is close to the expected value (cf. Fig. 2a). In the supermicrometer range, on the other hand, the average ratio between measured and calculated truncation is 0.71 for the three Radiance Research instruments tested, indicating that the nominal $Z(\Theta)$ overestimates the angular sensitivity of these nephelometers for coarse particles. Averaged over all particle sizes, the relative deviation between measured and calculated truncation is 29%.

In an attempt to reduce this deviation, the angular limits and the deviation from the ideal cosine response of the Radiance Research instruments was varied empirically until an optimum match between measured and calculated truncations was found for both submicrometer and supermicrometer test aerosols. The angular limits were varied symmetrically in both forward and backward scattering regions. Within the assumed angular limit, a hypothetical sensitivity curve $Z_x(\Theta)$ was constructed by exaggerating the TSI sensitivity curve $Z_{\mathrm{TSI}}(\Theta)$ of Anderson et al. (1996) by

$$Z_x(\theta) = Z_{\mathrm{TSI}}(\theta)(1 + \sin\theta)^X, \tag{4}$$

with $x \geq 0$. The optimized match for the Radiance Research instruments was found with angular integration limits of 15°–165° and $x = 0.1$. For this angular sensitivity the relative deviation between measured and calculated truncation sinks from 29% to 6%.

Applying the nominal angular limits and the manufacturers' angular sensitivity curve to the Ecotech instrument yields an average relative deviation between measured and calculated truncation of 39%. With the supermicrometer test aerosol of 1770-nm geometric mean size, the ratio of measured and calculated truncation was 1.52 (cf. Fig. 2b), indicating that the nominal $Z(\Theta)$ strongly underestimates the angular sensitivity of this nephelometer for coarse particles. The same empirical optimization as for the Radiance Research instrument was carried out for the Ecotech instrument yielding an increased effective angular range of 8°–172° and an amplification factor of the TSI sensitivity of $x = 0.35$. For this angular sensitivity the relative deviation between measured and calculated truncation sinks from 39% (nominal sensitivity) to 11%.

No claim can be made that the $Z_x(\Theta)$ for the two types of nephelometers are the correct ones, only that with these $Z_x(\Theta)$ the measured instrument response matches theoretical expectations for both submicrometer and supermicrometer test aerosols in an optimum way. The estimated angular response curves are substantially different from the nominal curves, and indicate that additional characterization of the optical geometry and response of the Radiance Research and Ecotech designs is needed. For the Ecotech instrument, the illumination with individual matched light-emitting diodes suggests the possibility of strong deviations from the ideal sine curve, with potential variations among individual instruments. However, fine-tuning of the LED outputs with this design has the potential to yield instruments that match the ideal angular response more closely than any of the other designs.

As a test of the validity of the empirical optimization of the angular response, the same procedure was applied to the TSI nephelometers. However, no improvement of the match between measured and calculated signals could be achieved by varying angular limits or sensitivities in the TSI instruments. When hypothetically varying the wavelengths of the TSI instruments an optimum match between measured and calculated submicrometer signals was found at a red wavelength of 770 nm, whereas no variation of blue and green wavelengths improved this match. This optimum exhibited nearly the same grand average relative deviation as given in Anderson et al. (1996). Average relative deviations between measured and calculated signals for this hypothetical spectral behavior of the TSI nephelometers are included in Table 3. The 770-nm wavelength is far outside the bandwidth of the red channel that was reported in Anderson et al. (1996). We do not claim that the wavelength response of the red channel in fact has its maximum at 770 nm, only that the unexplained deviations between measured and calculated signals in the red total channel can be compensated for by interpreting the red channel data at 770 nm without corrupting the match in supermicrometer aerosols.

TABLE 4. Average slopes, intersects, and coefficients of determination for all TSI model 3563, the three Radiance Research, and the Ecotech nephelometers for an intercomparison with ambient aerosols on 11–12 Nov 2003. The range of recorded data together with arithmetic mean is also given. As reference for the ambient statistics nephelometer TSI 1083 was taken. For the statistics of the non-TSI nephelometers spectrally interpolated reference data of TSI 1083 were used.

Parameter	TS blue	TS green	TS red	BS blue	BS green	BS red	RR 353	RR 408	RR ASF	Ecotech
Minimum (Mm^{-1})	56.4	42.6	28.2	7.1	5.8	4.4	63.6	40.9	38.2	41.8
Mean (Mm^{-1})	115	87.0	57.6	14.1	11.5	9.5	83.5	81.8	73.6	81.1
Maximum (Mm^{-1})	146	117	83.4	18.1	14.4	13.9	98.1	103	91.5	97.8
Slope	1.02	1.05	1.07	0.94	0.98	0.95	1.03	0.99	0.85	0.96
Intercept (Mm^{-1})	0.04	−0.19	0.25	0.36	0.08	0.53	−6.08	−4.47	−1.26	−3.94
R^2	0.99	0.99	0.99	0.94	0.97	0.94	0.98	0.98	0.98	0.98

d. Ambient aerosols

On the nights of 11–12 and 12–13 November 2003, all nephelometers were operated in parallel on ambient urban air taken from outside the laboratory, yielding 467 one-minute averages for comparison. The range of recorded data is given with the arithmetic mean for each instrument in Table 4. As in the laboratory experiments the following statistics are based on the TSI model 3563 number 1083 as independent variable. Average linear regression slopes, intercepts, and coefficients of determination are given in Table 2 for all nephelometers. For the TSI instruments, the average deviation of the slope from a 1:1 relation with TSI model 3563 number 1083 is less than 7%. Average intercepts range between +0.53 and −0.19 Mm^{-1}. Average coefficients of determination lie between 0.94 in the red backscattering channel and 0.999 in the green total scattering channel. In the former channel, the smallest scattering signals were measured.

For the Radiance Research and Ecotech nephelometers, the reference data (TSI model 3563 number 1083) were interpolated to the respective wavelengths of the individual instruments. Ambient regressions of the Radiance Research and Ecotech instruments with TSI model 3563 number 1083 show larger negative intercepts, which we attribute to their less well characterized optics and their lack of autocalibration with particle-free air.

6. Summary and conclusions

This study has determined measured and Mie-calculated signal truncations for total scatter (TS) and backscatter (BS) TSI nephelometers, as a function of wavelength and for both submicrometer and supermicrometer particles of known size and composition. The available aerodynamic measuring technique (APS) for liquid supermicrometer particles introduced an additional uncertainty that did not allow conclusive statements other than (a) the scattering data are 30% higher than calculated from APS with undersizing bias of zero, and (b) an APS undersizing bias of 20% brings the TS and BS measurements into agreement with APS results to within 5%. Rough empirical truncation corrections have been derived from the calibration data for the Radiance Research and Ecotech nephelometers.

To summarize the results of the experiments, expected signal truncations were calculated according to Eq. (3) for DEHS and plotted in Fig. 3 using the shape of the near-monodisperse size distributions of the test aerosols given in section 2b and by varying the geometric mean diameter between 100 and 10 000 nm. The general increasing truncations of nephelometer signals with increasing particle size shown in Fig. 1 was originally reported by Heintzenberg and Quenzel (1973b). At particle diameters >5 μm more than 50% of the light scattering coefficient is lost through angular truncation. Much smaller truncations are calculated for the backscattering signals. This is due to contamination of the backscatter channels with forward-scattered light,

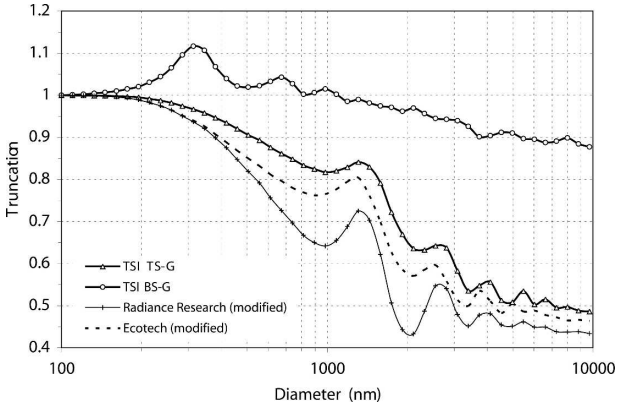

FIG. 3. Theoretical size-dependent signal truncations for DEHS aerosols with the average size distribution of the present study and the green total (TSI TS-G) and backscatter (TSI BS-G) channels in the TSI nephelometers, the empirically modified angular sensitivities of Radiance Research and Ecotech nephelometers. The truncations are normalized by the Rayleigh truncation to reflect the result of a gas calibration.

since the backscatter channels start measuring significantly below the nominal 90° angular limit (cf. Fig. 4b of Anderson et al. 1996). For the same reason, backscatter truncation values larger than one are calculated between 200- and 1000-nm particle diameter; that is, the nephelometer overestimates the backscattering of the respective particles by up to 11%.

For particles much smaller than the wavelength, the calculated truncations reach the Rayleigh limit of ≈0.98, that is, a ≈2% truncation, which applies to the calibration of the nephelometers with Rayleigh-scattering gases. It can be argued that a gas calibration results in the corresponding truncation being compensated if the instruments are tuned to read the corresponding Rayleigh-scattering coefficients. Alternatively, the instruments could be tuned to read truncated Rayleigh-scattering coefficients according to their angular response.

In Fig. 3 the modified Radiance Research characteristics exhibit the largest truncations because of their limited angular sensitivity. Starting with the nominal value of one at particle sizes ≪ wavelength, the ratio of truncation of the empirically modified Radiance Research nephelometer to TSI truncation sinks to a value of 0.9 at a particle diameter of 500 nm and reaches a minimum of 0.66 at 1900 nm, which explains the "enigma" of signal discrepancies between the two types of nephelometers as reported by Anderson et al. (2003). The modified Ecotech response leads to somewhat smaller truncations throughout the size range shown in Fig. 3 because of the empirically increased angular range. We emphasize that the empirical quantification of the angular response of the non-TSI nephelometers of the present study does not replace detailed experimental spectral and angular characterizations that are lacking for these instruments.

Acknowledgments. We gratefully acknowledge the German Federal Environmental Protection Agency (Umweltbundesamt) for supporting the World Calibration Centre for Physical Aerosol Parameters. Tad Anderson kindly provided spectral and angular calibration data for the TSI nephelometers and contributed substantially to the discussion of the results.

REFERENCES

Ackerman, T. P., and O. B. Toon, 1981: Absorption of visible radiation in atmosphere containing mixtures of absorbing and nonabsorbing particles. *Appl. Opt.,* **20,** 3661–3668.

Anderson, T. L., and J. A. Ogren, 1998: Determining aerosol radiative properties using the TSI 3563 integrating nephelometer. *Aerosol Sci. Technol.,* **29,** 57–69.

——, and Coauthors, 1996: Performance characteristics of a high-sensitivity, three-wavelength, total scatter/backscatter nephelometer. *J. Atmos. Oceanic Technol.,* **13,** 967–986.

——, D. S. Covert, J. D. Wheeler, J. M. Harris, K. D. Perry, B. E. Trost, D. J. Jaffe, and J. A. Ogren, 1999: Aerosol backscatter fraction and single scattering albedo: Measured values and uncertainties at a coastal station in the Pacific Northwest. *J. Geophys. Res.,* **104** (D21), 26 793–26 807.

——, S. J. Masonis, D. S. Covert, N. C. Ahlquist, S. G. Howell, A. D. Clarke, and C. S. McNaughton, 2003: Variability of aerosol optical properties derived from in situ aircraft measurements during ACE-Asia. *J. Geophys. Res.,* **108,** 8647, doi:10.1029/2002JD003247.

Baron, P. A., 1986: Calibration and use of the Aerodynamic Particle Sizer (APS 3300). *Aerosol Sci. Technol.,* **5,** 55–67.

Beuttell, R. G., and A. W. Brewer, 1949: Instruments for the measurement of the visual range. *J. Sci. Instrum.,* **26,** 357–359.

Charlson, R. J., J. Langner, H. Rodhe, C. B. Leovy, and S. G. Warren, 1991: Perturbation of the Northern Hemisphere radiative balance by backscattering of anthropogenic sulfate aerosols. *Tellus,* **43AB,** 152–163.

Collins, D. R., D. R. Cocker, R. C. Flagan, and J. H. Seinfeld, 2004: The scanning DMA transfer function. *Aerosol Sci. Technol.,* **38,** 833–850.

Dave, J. V., 1968: Subroutines for computing the parameters of the electromagnetic radiation scattered by a sphere. IBM Scientific Center, Palo Alto, CA, 65 pp.

——, 1969: Scattering of electromagnetic radiation by a large, absorbing sphere. *IBM J. Res. Develop.,* **13** (3), 302–314.

Ensor, D. S., and A. P. Waggoner, 1970: Angular truncation error in the in the integrating nephelometer. *Atmos. Environ.,* **4,** 481–487.

Hasan, H., and C. W. Lewis, 1983: Integrating nephelometer response corrections for bimodal size distributions. *Aerosol Sci. Technol.,* **2,** 443–453.

Heinicke, J., 1967: Measurement of light scattering in the near infrared and visible spectral region with two scattered light recorders (in German). M.S. thesis, Department of Meteorology, University of Munich, 65 pp.

Heintzenberg, J., 1975: Determination in situ of the size distribution of the atmospheric aerosol. *J. Aerosol Sci.,* **6,** 291–303.

——, and H. Quenzel, 1973a: Calculations on the determination of the scattering coefficient of turbid air with integrating nephelometers. *Atmos. Environ.,* **7,** 509–519.

——, and ——, 1973b: On the effect of the loss of large particles on the determination of scattering coefficients with integrating nephelometers. *Atmos. Environ.,* **7,** 503–507.

——, and R. J. Charlson, 1996: Design and applications of the integrating nephelometer: A review. *J. Atmos. Oceanic Technol.,* **13,** 987–1000.

Kasten, F., 1968: Rayleigh-Cabannes-Streuung in trockener Luft unter Berücksichtigung neuerer Depolarisations-Messungen. *Optik,* **27,** 155–166.

Marshall, I. A., J. P. Mitchell, and W. D. Griffiths, 1991: The behaviour of regular-shaped non-spherical particles in a TSI aerodynamic particle sizer. *J. Aerosol Sci.,* **22,** 73–89.

Masonis, S. J., K. Franke, A. Ansmann, D. Müller, D. Althausen, J. A. Ogren, A. Jefferson, and P. J. Sheridan, 2002: An intercomparison of aerosol light extinction and 180 ° backscatter as derived using in situ instruments and Raman lidar during the Indoex field campaign. *J. Geophys. Res.,* **107,** 8014, doi:10.1029/2000JD000035.

Ogren, J., 1995: *In situ* observations of aerosol properties. *Aerosol*

Forcing of Climate, R. J. Charlson and J. Heintzenberg, Eds., John Wiley and Sons, 215–226.

Quenzel, H., 1969: Der Einfluss der Aerosolgrößenverteilung auf die Messgenauigkeit von Streulichtmessern. *Gerlands Beitr. Geophys.,* **78,** 251–263.

Quinn, P. K., and Coauthors, 1996: Closure in tropospheric aerosol–climate research: A review and future needs for addressing aerosol direct shortwave radiative forcing. *Contrib. Atmos. Phys.,* **69,** 547–577.

Rabinoff, R. A., and B. M. Herman, 1973: Effect of aerosol size distribution on the accuracy of the integrating nephelometer. *J. Appl. Meteor.,* **12,** 184–186.

Ruppersberg, G. H., 1959: Recent approaches to recording the visibility on airports. Annual Report of the Scientific Society for Air Traffic, 230–236.

——, 1964: Registrierung der Sichtweite mit dem Streulichtschreiber. *Contrib. Atmos. Phys.,* **37,** 252–263.

Sheridan, P. J., A. Jefferson, and J. A. Ogren, 2002: Spatial variability of submicrometer aerosol radiative properties over the Indian Ocean during INDOEX. *J. Geophys. Res.,* **107,** 8011, doi:10.1029/2000JD000166.

Waggoner, A. P., N. C. Ahlquist, and R. J. Charlson, 1972: Measurement of the aerosol total scatter-backscatter ratio. *Appl. Opt.,* **11,** 2886–2889.

Wang, S. C., and R. C. Flagan, 1990: Scanning electrical mobility spectrometer. *Aerosol Sci. Technol.,* **13,** 230–240.

Wex, H., C. Neusüß, M. Wendisch, F. Stratmann, C. Koziar, A. Keil, A. Wiedensohler, and M. Ebert, 2002: Particle scattering, backscattering, and absorption coefficients: An in-situ closure and sensitivity study. *J. Geophys. Res.,* **107,** 8122, doi:10.1029/2000JD000234.

White, W. H., E. S. Macias, R. C. Nininger, and D. Schorran, 1994: Size-resolved measurements of light scattering by ambient particles in the southwestern U.S.A. *Atmos. Environ.,* **28,** 909–921.